Observing the Earth's magnetic field in an underground observatory: a case study from BFO

Rudolf Widmer-Schnidrig[1], Peter Duffner[2], Thomas Forbriger[3], and Walter Zürn[4]

1 Institute of Geophysics, Stuttgart University, Black Forest Observatory (BFO), Germany
E-Mail: widmer@geophys.uni-stuttgart.de
2 Geodetic Institute, Karlsruhe Institute of Technology, Black Forest Observatory (BFO), Germany
E-Mail: peter.duffner@kit.edu
3 Geophysical Institute, Karlsruhe Institute of Technology, Black Forest Observatory (BFO), Germany
E-Mail: thomas.forbriger@kit.edu
4 retired, Black Forest Observatory (BFO), Germany
E-Mail: walter.zuern@partner.kit.edu

1 Introduction

While we humans have no sensory ability to perceive the Earth's magnetic field its presence has a number of important consequences which make it a worthwhile object of study. On the one hand it protects life in the biosphere from harmful solar and cosmic radiation and on the other hand prevents the erosion of the atmosphere by solar wind. The magnetic field has also important technical applications such as navigation based on a magnetic compass. To understand the processes by which the Earth's magnetic field is generated we study its long-term temporal variation. These variations provide us with a window through which we can study the dynamo which is thought to be driven by thermal convection in the Earth's liquid outer core and which in turn is responsible for the steady regeneration of the magnetic field.

Convective velocities in the outer core are large compared to the velocities of mantle convection: centimeters per minute as opposed to centimeters per year. Expressed in terms of every day life: the speed of a snail as opposed to the speed with which human hair grows. In spite of the higher velocities in the core the resulting variations in the Earth's exterior magnetic field take place over decades and centuries. So to observe these slow variations utmost care must be taken to limit or at least to capture instrumental drift.

At typical geomagnetic observatories instrumental drift of the continuously observing variometers is addressed by conducting frequent (weekly) observations of the magnetic field with so called absolute instruments: a theodolite with a flux gate sensor mounted on top of the telescope and a scalar magnetometer for the total field strength. The absolute measurements with a theodolite require a well trained human observer. One obtains the inclination and declination of the magnetic field and together with a total field measurement obtained with an Overhauser magnetometer those allow to fully specify the magnetic field vector at the time of the observation. By comparing the absolute measurement with the data from the continuously recording 3-component variometer we infer instrumental drift over weekly and longer time scales. Experience at many observatories has shown that these drifts are due to an inherent temperature sensitivity of the flux gate sensors and due to tilting of the pillar on which the variometer rests (caused by solar heating of the soil surrounding the magnetics hut or by reaction of the soil to precipitation).

At BFO we operate a geomagnetic observatory and one aim of this article is to describe the technical solutions

Erschienen bei KIT Scientific Publishing
Schriftenreihe des Studiengangs
Geodäsie und Geoinformatik 2018,1

DOI Einzelbeitrag:
10.5445/KSP/1000080251

Festschrift zur Verabschiedung von
Prof. Dr.-Ing. Dr. h.c. Bernhard Heck
(Schw)Ehre, wem (Schw)Ehre gebührt

DOI Festschrift:
10.5445/KSP/1000080324

that we have come up with in setting up such an observatory overcoming the above mentioned problems.

2 History

Ever since the inception of BFO the observation of the Earth's magnetic field belonged to its tasks. The activities in this field started simultaneously with the construction of the main laboratory building: a separate hut dedicated to magnetic observations was constructed 200 m away from the laboratory (fig. 2.1). This hut had to be magnetically clean. Hence it got a Eternit roof, wooden walls and only brass screws were utilized in its construction. The initial expertise to install and operate a magnetic observatory came from our colleagues Martin Beblo and Martin Feller of the geomagnetic observatory Fürstenfeldbruck (FUR) who at the time were interested to run BFO as a magnetic outpost of FUR for redundancy and for data quality checks.

In 2000, with the arrival of one of the authors (R.W.-S.) at BFO, it was decided to upgrade the installed hardware with modern, state-of-the-art sensors and data acquisition systems with the goal of becoming an INTERMAGNET observatory. INTERMAGNET is an international association of geomagnetic observatories that sets the de-facto standard for the terrestrial observation of the Earth's magnetic field. INTERMAGNET archives and disseminates magnetic observatory data in a standardized form and is the primary source of data used to constrain models of the Earth's magnetic field. By becoming a member of INTERMAGNET we also anticipated that the data from BFO would get the widest possible usage by the global research community. Observations with the new hardware started in January 2003 and in 2006 – after evaluation of the quality of its magnetic data – BFO was awarded the status of an official INTERMAGNET magnetic observatory (IMO).

3 Sensors

The signal to be observed in geomagnetism covers the frequency band from DC to 1 Hz. Of course the magnetic spectrum does not stop at 1 Hz but higher frequency magnetic field variations do not penetrate deep into the Earth. They are the interest of magnetotellurics (0.01 Hz - 10 kHz) or georadar (25 MHz - 2.5 GHz).

At least two disciplines that are prominently represented at BFO share a common interest in the zero-frequency (DC) field value: gravimetry and geomagnetism. This interest in the long term field variations sets these two disciplines apart from seismology - a third discipline prominently represented at BFO. The frequency band of interest for seismology stops at the frequency of the Earth's gravest seismic free oscillation, the spheroidal mode ${}_0S_2$ with a frequency of 0.3 mHz (Häfner and Widmer-Schnidrig, 2012). There is no scientific interest for a seismometer with sensitivity at lower frequencies.

In instrument design high dynamic range and high sensitivity seem to be two competing design goals. At least in magnetics and in gravimetry there is still no sensor which achieves both these goals at the state-of-the-art levels. The approach taken by these two communities is to build and operate two distinct sets of sensors: one in which the sensitivity is maximized and the other in which the magnitude of the field can be observed. This is a viable solution because for both disciplines the signal to be observed consists of a large DC signal and a superposed variation that is small compared to the DC part: $\sim$1% in the case of the magnetic field and $\sim$1ppm in the case of the gravity field.

In gravimetry the two complementary types of instruments would be the free fall absolute gravimeter measuring the magnitude of Earth's gravity, g, to 1 part in 10^9 and the super conducting gravimeters or the LaCoste-Romberg spring gravimeters measuring variations with a resolution of $10^{-12}g$.

In magnetics the absolute instruments are the Proton Precession Magnetometers (PPM) or Overhauser magnetometers (fig. 3.1) which measure the magnitude of the magnetic field vector and the DI-flux theodolite (fig. 3.2) measuring the absolute value of the declination (D) relative to geographic North and the inclination (I) relative to the horizontal as defined by the local gravity. Small variations in the vector components of the magnetic field are observed continuously with a three component fluxgate magnetometer - a so called vector magnetometer.

Figure 3.1: The Overhauser GSM-90 sensing unit installed in the upper tunnel of the Anton mine. The white cover (seen on the left) has been removed for the picture.

Continuing the comparison with neighboring disciplines we compare the dynamic range and the bandwidth of signals to be recorded at INTERMAGNET observatories and at stations of the Global Seismic Network (GSN) in table 3.1. Signals in geomagnetism cover a larger bandwidth while signals in global seismology cover a larger dynamic range. Since BFO is one of only very few observatories where both disciplines are actively pursued, the observatory offers a unique opportunity where expertise brought together from these two disciplines can benefit from each other.

Table 3.1: Comparison of signals to be recorded at geomagnetic and seismologic global observatories: bandwidth (BW) and dynamic range (DR).

	INTERMAGNET observatory	Global Seismic Network
BW	century^{-1} - 0.1 Hz 9 decades	0.3 mHz - 30 Hz 5 decades
DR	0.5 - 50000 nT 100 dB	10^{-12} - 10^{-5} m/s^2 140 dB

3.1 Overhauser scalar magnetometer

Sensors used to measure the magnitude of the magnetic field vector $F = |\vec{B}|$ are referred to as scalar magnetometers. At BFO we use an Overhauser GSM-90 magnetometer from GemSystems (Ontario, Canada). In this sensor the Larmour frequency of the proton Ω_L is measured. This is the frequency with which the magnetic moments of isolated protons (nucleii of hydrogen atoms) precess around the magnetic field vector. The Larmour frequency is strictly proportional to the magnitude of the magnetic field with the gyromagnetic constant $\gamma = 4.257 \cdot 10^7$ Hz T^{-1} as proportionality factor. Thus for a field of ∼48000 nT the Larmour frequency is $\Omega_L \simeq 2.05$ kHz. A frequency measurement

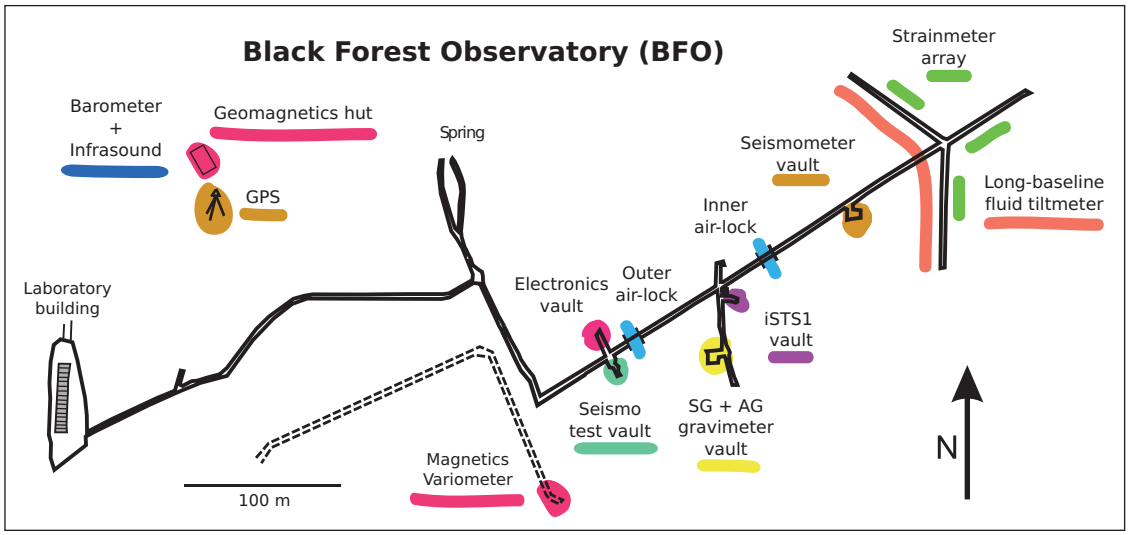

Figure 2.1: The underground tunnels of the Anton mine. It consists of two levels: lower and approx. 700 m long gallery (solid lines) and a shorter, 200 m long upper tunnel (dashed lines). The two systems are vertically separated by 60 m. The magnetic variometers (fluxgate and Overhauser sensors) are located at the end of the upper level gallery system. The DI-flux theodolite is housed in the magnetics hut to the North-East of the laboratory building. The overburden at the end of the lower tunnel is 170 m and at the end of the upper tunnel 50 m.

is made every 5 seconds - more rapid measurements would not yield the desired accuracy.

Since the gyromagnetic constant is a property of an elementary particle it is independent of environmental parameters such as the temperature or atmospheric pressure. As such it is perfectly suited for an absolute, DC stable measurement. The only point of concern is the frequency stability of the oscillator against which the Larmour frequency signal is measured.

Figure 3.2: At BFO the DI-Flux theodolite is a non-magnetic Zeiss Theo-020 theodolite with a brass covered fluxgate sensing unit mounted on top of the telescope.

3.2 DI-flux theodolite

To determine the orientation of the magnetic field vector we use a non-magnetic theodolite Theo-020 from Zeiss (Jena) (fig. 3.2) that we have on loan from Fürstenfeldbruck observatory. The theodolite is installed in the magnetics hut 200 m to the North-East of the main laboratory building (fig. 3.3). The smallest angular subdivision on the reading scales are 1/3 of a minute of arc so that readings down to 1/10th of a minute are possible. The single-component fluxgate magnetometer is a Mag-01H from Bartington. The digitally displayed field values on the electronics unit are updated twice per second with 0.1 nT being the least significant digit. With a background field at BFO of $\sim$48000 nT and an inclination of $\sim$64° the magnetometer reading changes by 13.8 and 6.1 nT per minutes of arc for inclination and declination measurements respectively. Thus in the case of our DI-flux theodolite the angular resolution of the theodolite is the limiting element for the overall precision of the inclination measurements. The declination also depends on the quality with which we can know the direction of geographic North. As we shall see below (sec. 5.1) this direction is only known to within 1 minute of arc, which must be taken as the uncertainty in the estimated declination.

The procedure involved in an absolute measurement of the declination and inclination is described below in Section 5.1.

Figure 3.3: Magnetics hut and the tripod supporting the permanent, geodetic quality GPS antenna *BFO1*. The hut houses the DI-flux theodolite, a barometer, an infrasound sensor and a combined temperature-humidity sensor. Peter Duffner is seen during maintenance work on the GPS antenna.

3.3 Fluxgate vector magnetometer (variometer)

Our FGE fluxgate magnetometer is manufactured by the Danish Meteorological Institue (DMI) in Copenhagen. It is built around a cube of Carrara marble (fig. 3.4). On three sides a V-shaped groove holds the fluxgate sensors in an orthogonal arrangement. The marble cube sits on an aluminum base plate that can be leveled. We have chosen to install the permanently recording magnetometers in the upper tunnel of the

Anton mine. This part of the mine did not house any permanently installed instruments up to that point. This had the disadvantage that we first had to bring power and optical fibers for data transmission into this part of the mine. The advantage however was, that this part of the mine was magnetically clean: no iron hardware from prior experiments was installed in that section of the mine: such potentially magnetic objects are a major concern when selecting an installation site for a variometer.

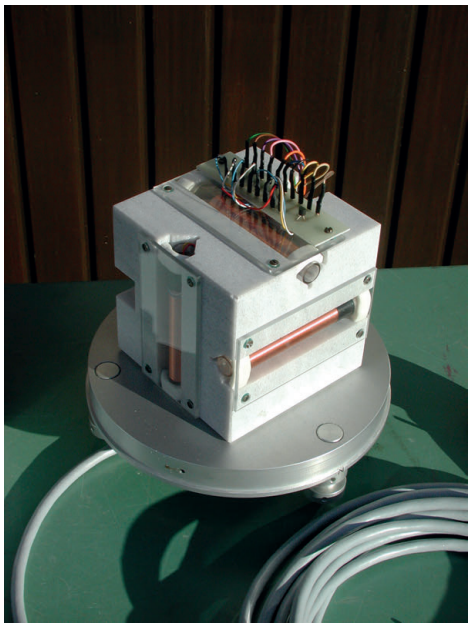

Figure 3.4: The FGE fluxgate magnetometer prior to installation in the mine. The white marble cube holds the three fluxgate sensors.

Figure 3.5: The FGE fluxgate magnetometer installed in the mine. Through the transparent plastic cover the sensor and a bag full of orange colored desiccant can be seen.

In the mine the FGE is installed on a polished granite slab that has been glued to a concrete pier sitting on the granitic floor. On top of the sensor we placed a glass bowl filled with desiccant and everything is covered by an upside down transparent bucket (fig. 3.5) so that we can visually inspect the state of the desiccant and hence are able to monitor the humidity underneath the bucket without touching the variometer. The feedback electronics of the fluxgates is housed 15 m away in the electronics cabinet (fig. 4.2).

4 Data acquisition

4.1 Buffer amplifier

The electronics unit of the FGE fluxgate provides the output signals of the three sensors as single-ended, analog voltages. Wires transporting such signals are susceptible to picking up stray EM fields. For this reason differential signals are preferable over single-ended signals. To address this shortcoming of the FGE electronics we built a buffer amplifier which low-pass filters the signal with a second-order Bessel low-pass (f_c=20 Hz) and inverts it to deliver a differential signal on output. The low-pass filter is added to suppress any harmonics from the power grid as well as other spurious signals from the nearby digital electronics. The design used for the buffer amplifier is actually taken from the one we built to interface our superconducting gravimeter with a seismic data acquisition system: the Q330HR (Forbriger, 2011).

4.2 Digitizer

To acquire data from the geophysical sensors at BFO the 26bit Q330HR digitizers from Quanterra have been selected. These are digitizers designed for the particular needs of seismology: signals with high dynamic range but no particular need for DC stability (see table 3.1). However, the suitability of the Quanterra Q330 digitizer for use with a superconducting gravimeter - where DC stability is of paramount importance - has been investigated by Van Camp et al. (2008). Combining their findings with the characteristics of the FGE magnetometer signal we concluded that the 24bit Q330 is perfectly suited for acquiring the FGE data.

The principal concern with using a seismic data acquisition is related to the automatic self-calibration after every digitizer reboot. The voltage reference used for this self-calibration exhibits some undesirable temperature dependence. However, since we operate the Q330 in a thermally stable environment these - hopefully rare steps - are expected to be too small to be noticeable in the data. In fig. 4.1 the digitizer self-noise is plotted together with the FGE signal and the former is ∼50 dB below the magnetometer signal. This large 50 dB margin also absorbs the unwanted steps introduced into the signal by the self-calibrations.

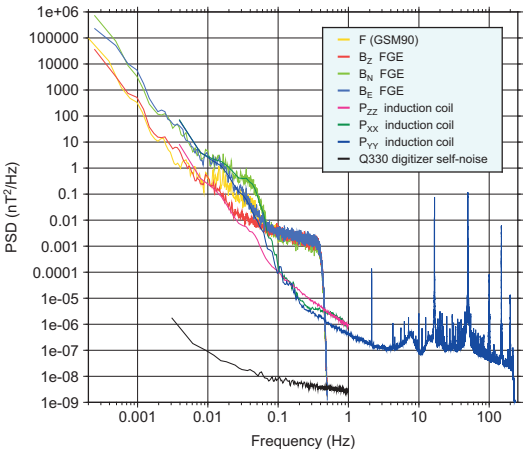

Figure 4.1: Observation of the magnetic field at BFO from 8.-9. Dec. 2016 with different sensors: the fluxgate FGE and Overhauser GSM-90 resolve the low-frequency part of the spectrum while the induction coils cover the band from 1000 seconds to kH frequencies. Burried underneath many narrow technical spectral lines is the broad peak of the lowest-order Schumann resonance at 7 Hz. For clarity only one horizontal field component is plotted at frequencies above 1Hz. The induction coils were operated in the upper tunnel of the Anton mine. The noise-floor of both the FGE fluxgate and the Overhauser are around 0.003 nT^2/Hz. The self-noise of the Q330 digitizer is ∼50 dB below the FGE fluxgate signal.

4.3 Timing of acquisition: GPS and NTP

Nowadays the preferred way to synchronize the clock in data acquisition systems world wide is based on the Global Navigation System GPS. Together with precise geographic coordinates each GPS receiver necessarily also knows the time: for a position with a ∼10 m error the time must be known to within ∼30 nanoseconds. This is how long it takes for an electromagnetic wave to travel a distance of 10 m. Is a 30 ns time jitter small enough to not lead to any signal degradation? What is the timing requirement for the signal we want to record? To give a quantitative answer to this question let us assume that we want to record a monochromatic sine wave with maximum amplitude and maximum frequency. The variometer signal saturates for signals larger than $A = \pm 1000$ nT (see above) and is being recorded with 1 sample per second. Thus the Nyquist frequency is f=0.5 Hz. Our hypothetical signal y then is $y(t) = A\sin(2\pi ft)$. The rate of change of the signal amplitude is $dy/dt = 2\pi fA\cos(2\pi ft)$ and its largest value is $dy/dt = 2\pi fA$. With this expression we can relate a time jitter dt to a jitter in the signal amplitude dy and vice versa. A jitter of dt=30 ns from the GPS clock thus translates to an amplitude jitter of dy =0.1 pT, a value 100 times smaller than the least significant digit reported to INTERMAGNET. To stay below the 10pT bit-noise of the INTERMAGNET-1s data standard a time jitter smaller than 3 μs are needed. However, in a mine setting we have no reception of the GPS signal and absolute time to within 30 ns is not available. To remedy this shortcoming we came up with the technical solution described below. In the laboratory building we operate a GPS disciplined clock that can maintain a stable time reference even during outages of the GPS signal: its internal oscillator drifts by less than a second in a year. This clock - a Meinberg GPS167 - outputs a pulse-per-second (PPS) signal where the leading edge of the pulse is precisely synchronized to the beginning of the second. The same clock also outputs time telegrams every second with the absolute time information of the most recent PPS pulse. This information: the time telegram and the PPS pulse is also what the Q330 data acquisition can accept from an external source in order to stay synchronized with absolute time. To transport the time information into the mine we use dedicated multimode 50/125 μm optical fibers for the PPS pulses. For the absolute time information we use the Network Time Protocol (NTP) with which PCs connected to a computer network can stay synchronized. Two PCs connected to the BFO computer network are needed: an NTP time server located next to the GPS167 clock and from which it gets the time and a PC located next to the Q330 digitizer acting as NTP-client. The latter PC outputs the time telegrams suitable for the Q330 digitizer. We have found that the NTP time jitter in our computer network is below 10 ms which is good enough to correctly time tag the PPS pulses. The quality of the Q330 timing is then only limited by the travel time of the PPS through the fiber (∼5 μs) and the ∼100 ns rise time of

the optical-electrical media converters. The former is a constant time delay that is negligible for the interpretation of the magnetic signals. The 100 ns rise time is a conservative estimate of the time jitter and is well below the above mentioned 3 μs minimum requirement to reach a 10 pT resolution. A detailed description of the technical implementation at BFO is given in Forbriger (2013).

4.4 Recorder

To interface with the Q330 digitizer we operate a mini-PC running Linux. Once every second it sends a current time telegram (as mentioned above) and simultaneously receives the digital fluxgate data. The software used to handle the real-time data flow is Seiscomp-2.6 with the Seedlink protocol (Hanka et al., 2000, 2010). This data is locally stored in a disk loop and transferred to a central server in the laboratory building before going to Niemegk and eventually to the INTERMAGNET data servers. The same mini-PC also communicates with the Overhauser GSM90 electronics and triggers each of its measurements.

Figure 4.2: Electronics cabinet (with the cover removed) in the upper tunnel of the Anton mine. It houses the electronics units of the FGE and Overhauser magnetometers, the Q330 digitizer, the buffer amplifier, fiber optic media converters for LAN and PPS signals, a mini-PC, a Hygrometer and power supplies.

Except for the sensor heads, all the magnetics hardware in the mine is tightly packed in a sealed cabinet where it is protected from the very high humidity (fig. 4.2).

For reasons of redundancy the Q330 directly interfaces also with a second PC in the laboratory building running FreeBSD operating system and the Near-Real-Time-System (NRTS) software by the IRIS/IDA (Incorporated Research Institutions for Seismology) group in San Diego. The data passing through this system is forwarded to the IRIS/DMC in Seattle (USA) where it is also made publicly available with a typical delay time of under 30 seconds.

Table 4.1: Calibration of stages along the FGE variometer signal path.

stage	sensitivity, gain
FGE fluxgate	100 nT/V
buffer amplifier	2x gain
Q330 digitizer	2.38 μV/count
overall	8388.6 counts / nT

5 Applications

5.1 Absolute measurements with a DI-flux theodolite

Absolute measurements of the declination and inclination of the magnetic field still require a human observer: devices capable of automatic absolute measurements are still at the prototype stage. Here we describe briefly the procedure of conducting such an absolute D, I - measurement.

To start out a tie to the geographic coordinate system is established by pointing the cross-hair of the telescope at two geographic targets 60 - 80 m away. The azimuth of these targets relative to geographic North was established with a gyrocompass to within one minute of arc by Klaus Lindner (GIK, KIT) in 2004. In a second step the telescope is leveled and turned around the vertical axis until the fluxgate reads zero field strength. The local magnetic meridian plane is oriented perpendicular to this direction and so is the horizontal component of the magnetic field, $\vec{H}$. The declination D is the angle in the horizontal plane between geographic North and $\vec{H}$. In a third step the inclination I is determined by rotating the telescope in the plane of the magnetic meridian until the fluxgate reads again zero field strength. The telescope is now perpendicular to the magnetic field vector and the inclination I of the magnetic field is exactly 90° away from the inclination of the telescope.

Since the optical axis of the telescope and the sensitive axis of the fluxgate sensor are not perfectly aligned, the above measurements are repeated once with the fluxgate sensor above the telescope and once below. For the repeat measurements the telescope is pointing in all four directions: East and West for measuring the declination, North and South for the inclination. With the eight resulting readings the misalignments (also called collimation angles) can be estimated simultaneously with the inclination I and declination D of the magnetic field. The collimation angles are a property of the theodolite and should not change from one DI-flux measurement to the next so that the scatter in these values (fig 5.1, top panel) can be taken as a measure of uncertainty in the absolute observations: they typically change by less than $0.2'$ between successive observations.

The definition of the collimation angles in fig. 5.1 assumes that the axis of the telescope is horizontal. Then the displayed quantities in the top panel of fig. 5.1 are the misalignment between optical and magnetic axes in the vertical plane ε_H, ε_V and in the horizontal plane δ_H (Jankowski and Socksdorff, 1996). ε_H, ε_V denote the same angle: once computed from the four declination measurements (subscript H) and once from the four inclination measurements (subscript V). The middle panel shows the zero offset So_H and So_V of the fluxgate sensor together with the room temperature in the magnetics hut. The room temperature and the sensor offset are clearly anti correlated: a well known problem with fluxgate sensors that is mitigated by the above measurement strategy.

If we combine inclination I and declination D obtained from the theodolite readings with the simultaneously recorded total field F we can predict the components of the magnetic field vector $\vec{B}$:

$$\begin{aligned} B_x &= F\cos(I)\cos(D) \\ B_y &= F\cos(I)\sin(D) \\ B_z &= F\sin(I) \end{aligned} \qquad (5.1)$$

Taken together with the variations $x(t), y(t)$ and $z(t)$ provided by the fluxgate variometer we can estimate the baseline values as defined in eq. 5.2. These are shown in the bottom panel of fig. 5.1. Over a time span of seven years the baseline value for X (North) increased by 6 nT while Z (Vertical) decreased by 2 nT. The tendency in the Y (East) baseline is less clear.
What could be the reason for the very slow but steady variation of the baselines in the bottom panel of fig. 5.1? A tilting of the FGE fluxgate magnetometer towards the North-East by an angle of $9''$/a or 1° in 380 years could explain the behavior of the X_B (= North) and Z_B (= vertical) component base line values. We can only speculate what could be responsible for such a tilt: bulging of the concrete pillar or bulging of the glue between pillar and granite base-plate, which are both exposed to 100% humidity.

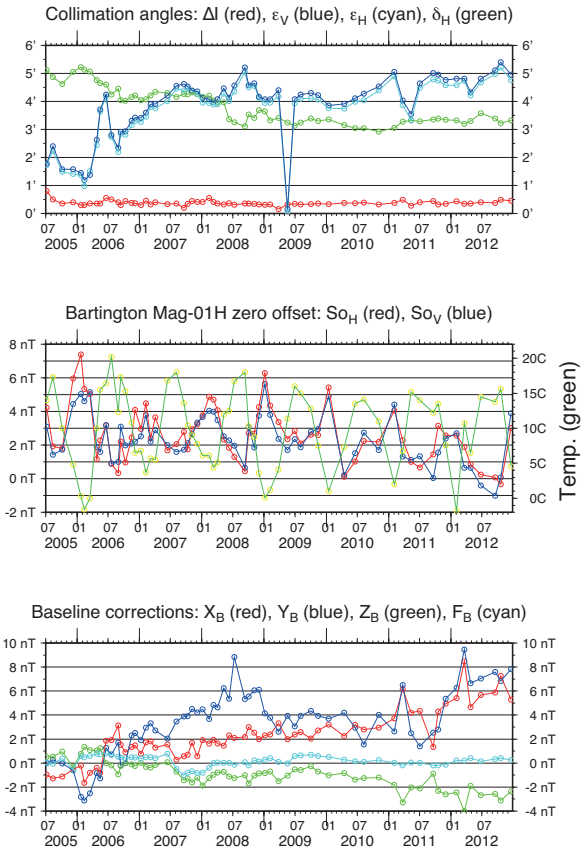

Figure 5.1: Summary plot of 62 absolute measurements taken between 2005 and 2012. The top panel shows the variation of the collimation angles. The middle panel shows the zero-offset of the fluxgate sensor mounted on the theodolite together with the room temperature in the magnetics hut. The bottom panel shows the evolution of the baseline values.

The stability of the baseline values is a measure of the instrumental drift of the variometer. Since such a baseline drift can mimic a slow variation of the magnetic field the baseline drift is monitored with DI-flux absolute measurements. Unstable baselines require more frequent absolute measurements whereas very stable baselines require less frequent observations. We have taken the small drift of the variometers as documented

in figures 5.3 and 5.4 together with the small baseline scatter documented in fig. 5.1 as justification to increase the time between DI-flux measdurements from weekly to once every six weeks.

5.2 Data quality – consistency check of vector against scalar magnetometer

Instrumental drift of the variometer can be checked by comparing the vector field measurements with the data from the Overhauser PPM magnetometer. The latter records $F = |\vec{B}|$ where $\vec{B} = (B_x, B_y, B_z)^T$ is the magnetic field vector.
The FGE fluxgate does not record the individual components of $\vec{B}$ but only their variations $x(t)$, $y(t)$, $z(t)$:

$$\begin{aligned} B_x(t) &= X_B + x(t) \\ B_y(t) &= Y_B + y(t) \\ B_z(t) &= Z_B + z(t), \end{aligned} \tag{5.2}$$

where X_B, Y_B, Z_B are the so called baseline values. Since variations in B are small we can linearize the relation between variations in F and variations in the components X, Y and Z

$$|\vec{B(t)}|^2 = [F + \Delta F(t)]^2$$

so that to first order

$$\Delta F(t) = \frac{X_B}{F} \cdot x(t) + \frac{Y_B}{F} \cdot y(t) + \frac{Z_B}{F} \cdot z(t) + C_0, \tag{5.3}$$

where C_0 is a constant offset from the contribution of the unknown fluxgate sensor offsets. This system linearly relates for any instant in time variations in $\Delta F(t)$ with variations in the vector components $x(t)$, $y(t)$ and $z(t)$. Given long time series of F, x, y and z the scale factors $c_x = X_B/F$, $c_y = Y_B/F$, $c_z = Z_B/F$ and offset C_0 can be estimated by solving eq. 5.3 in a least squares sense.
If the variometer signals x, y, z are calibrated and converted to nanoteslas like the Overhauser signal then the coefficients c_x, c_y, c_z are simply the directional cosines obtained from projecting the magnetic field vector onto the coordinate axes. This can be used to check the consistency of the calibration: the L_2-Norm of $c = (c_x, c_y, c_z)^T$ should be unity.
This check has been conducted most recently with the data from January 2014 to September 2017 and we found $c = 0.9994$ - thus it looks like the acquisition chain consisting of fluxgate, buffer amplifier and Q330 digitizer is calibrated to better than one part in 10^3.

This conclusion cannot be drawn for all three fluxgate components: the component which points East contributes very little to the total field variatons. This is because the magnetic declination at BFO is currently very small ($D \simeq 2^\circ$).

In anticipation of the shortcoming of such a calibration check we have operated the FGE fluxgate magnetometer from 2003 to 2012 in a unconventional orientation: the X-component was pointing North-East while the Y-component was pointing North-West. In such a configuration all three fluxgate sensors contribute with similar weights to variations in F and a baseline drift of any one component would show up in the consistency check of the calibration.

The residue from solving eq. 5.3 for the two fluxgate installations is shown in fig. 5.3 for the FGE setup prior to 2013 and in fig. 5.4 for the reoriented sensor after 2013. The residual variations are below 2 nT for both installations. The cause of these slow variations are unknown. If they came from the environment we would first of all expect to see seasonal temperature variations, which we don't. We can only speculate that it is due to an instability in the FGE electronics, its power supply or - less likely - in the frequency standard of the GSM90. To safely exclude the latter possibility a calibration of the GSM90 should be made, as this has not been done ever since we installed it in 2003.

The salient point of this section is, that even without applying time variable baseline corrections the consistency check realized in eq. 5.3 finds only very small deviations. Variations below 5 nT (after applying baseline corrections) are the target value for INTERMAGNET observatories. Our guess is that the stable environment provided by the installation in the Anton mine is primarily responsible for this low instrumental drift: stable ambient temperature and mechanically stable instrument pier.

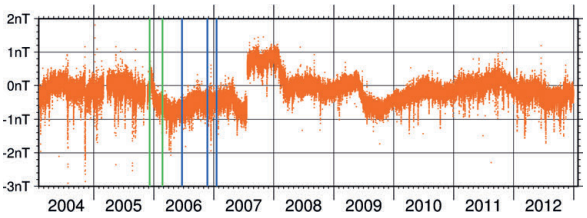

Figure 5.3: The vector of residues from solving eq. 5.3 for the years before the Q330 was installed. Note: the target for INTERMAGNET observatories is to have baseline variations below 5 nT. The vertical lines indicate times where the scalar magnetometer was moved and a small offset was introduced. The shown data has these offsets removed.

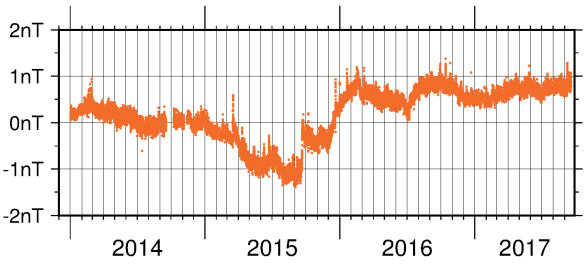

Figure 5.4: The vector of residues from solving eq. 5.3 since the Q330 digitizer was installed.

5.3 Frequency calibration of variometer

We conducted a calibration experiment to determine the transfer function of the FGE variometer. The focus of this experiment was to determine the frequency response at high frequencies. At low frequencies the calibration can be checked against the Overhauser. In order not to mechanically disturb the FGE sensor we placed a pair of calibration coils from an Askania torsion balance magnetometer next to the FGE. Using a battery as power source we applied voltage steps to the calibration coils. In the lines to the coils we had a resistor inserted and the voltage drop over this resistor was recorded on a free channel of the Q330. In this way we have a measure of the applied current flowing through the coil and hence the added magnetic field from the coil together with the response of all three fluxgate sensors: input and output to the varimeter are thus known (fig. 5.2).

Using the CALEX software (Wielandt, 2012; Wielandt and Forbriger, 2016) to analyze these signals (recorded at 40 samples per second) we find that the transfer function can be described by a first order low-pass filter with a corner frequency at 1.8 Hz. This is in agreement with the specifications of the manufacturer and confirms that the response of the variometer, when recorded at 1 sample per second can be considered as being independent of frequency.

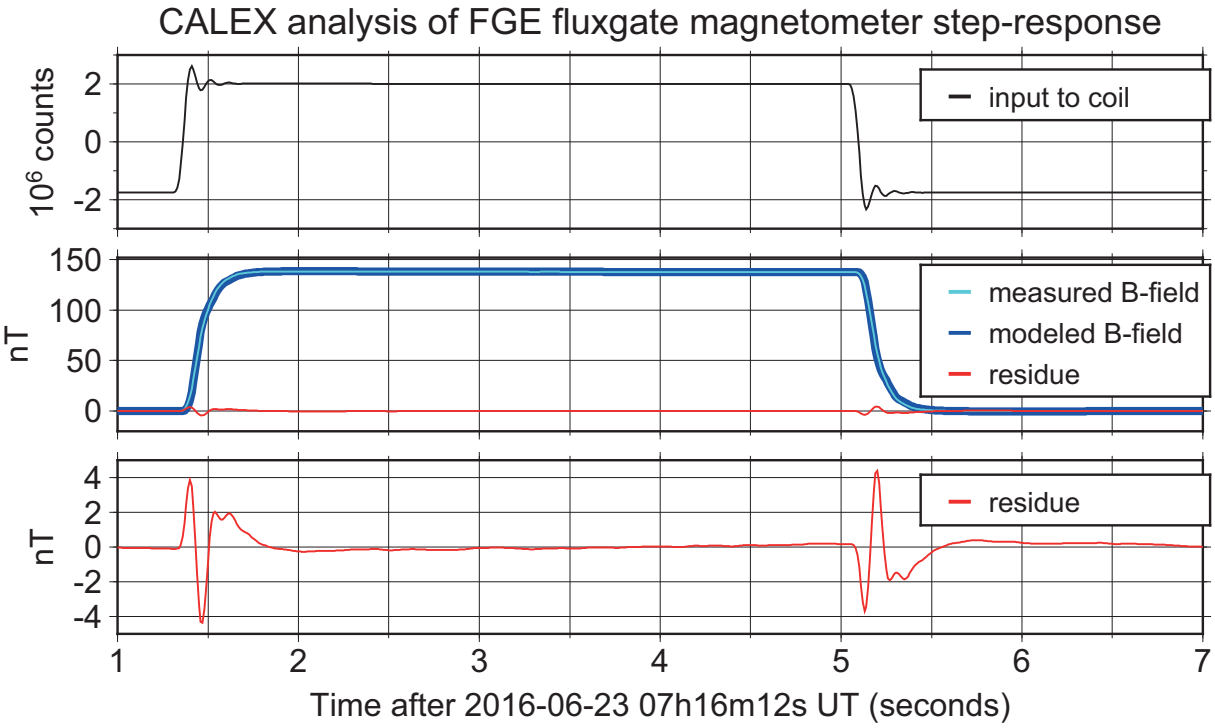

Figure 5.2: Experimental frequency response determination of FGE fluxgate magnetometer. The top panel shows the current flowing through the coils. The middle panel shows the observed output overlain by the modeled output: the two are indistingushable at this scale. The bottom panel shows the difference between modeled and recorded fluxgate output. Note the 30 times smaller scale on the axes.

5.4 Magnetic sensitivity of broad-band seismometers

In this section we give an example of how observations in the two disciplines, seismology and geomagnetism, are closely linked at BFO. Operating sensors from both disciplines we noticed repeatedly that magnetic storms show up in recordings of broad-band seismometers (Klinge et al., 2002; Forbriger, 2007; Forbriger et al., 2010). In fig. 5.5 such an event is documented. A teleseismic earthquake recorded on all three components of the STS-2 seismometer at BFO is shown (blue). Shortly after the initial Rayleigh waves have passed a large low-frequency disturbance is visible. It coincides with a magnetic field disturbance due to a solar coronal mass ejection (CME). A linear combination of the scaled magnetograms (red) almost perfectly reproduces these low-frequency disturbances which can now be subtracted to get a cleaned seismogram (not shown). The sensitivities to magnetic field variations is given in the figures: 0.390, 0.367 and 0.060 (nm/s^2)/nT for the East, North and vertical components, respectively.

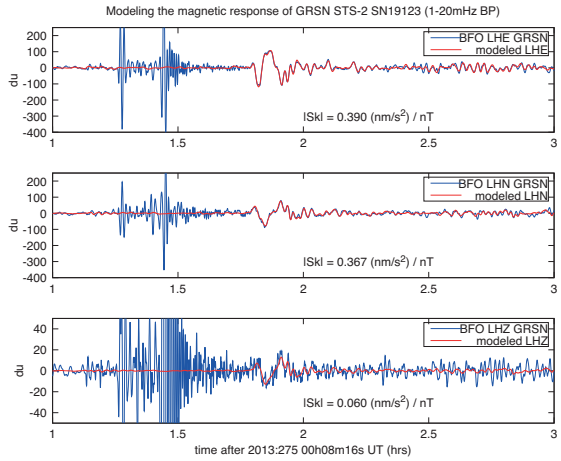

Figure 5.5: Modeling parasitic magnetic signals in broad-band seismograms. Seismograms (in raw counts: du) are shown in blue and magnetograms in red. The latter have been convolved with the instrument response of the STS-2 seismometer. A linear combination of the scaled magnetograms (red) almost perfectly reproduces these low-frequency disturbances which can now be subtracted to get a cleaned seismogram (not shown).

5.5 Carrington event

Having demonstrated that broad-band seismometers exhibit some parasitic magnetic sensitivity and having seen in fig. 5.5 that the influence of magnetic field variations on broad-band sensors can be deterministically treated, we now look at a very unlikely yet dangerous event: a very large geomagnetic storm, a so-called Carrington event (named after Carrington who documented the geomagnetic storm of Sept. 1st 1859), and ask how our magnetometers and seismometers would perform when confronted with such a signal.

The FGE fluxgate magnetometer outputs an analog voltage signal in the range ± 10 Volts. As next stage the buffer amplifier with gain 2x is operated with ± 15 Volts. Its output saturates if the input exceeds ± 30 Volts or ± 3000 nT. The last stage is the digitizer: it can take ± 20 Volts on input. Thus neither the buffer amplifier nor the digitizer limit the dynamic range coming from the fluxgate magnetometer.

To put these numbers into perspective we note that the magnetic storm of October 28th 2003 had an amplitude at BFO of 800 nT in the E-W-component and was only 20% below the clipping level of the FGE magnetometer.

How would the Streckeisen STS-2 seismometer perform as a magnetometer? In Forbriger (2007) it was shown that the magnetic field acts like a force on the seismometer mass or equivalently like a ground acceleration. The sensitivity of the STS-2 at BFO was estimated to $\sim$0.4 (nm/s^2)/nT for the horizontal components and $\sim$0.06 (nm/s^2)/nT for the vertical component. The manufacturer specifies that for a signal period of 33 seconds the STS-2 will clip for accelerations of 0.00055 g or 0.0055 m/s^2. Thus the next Carrington event can be $\sim$100 times stonger than todays magnetic field of 48000nT before the STS-2 will clip. Of course a low-gain magnetometer should be preferred to record such a huge magnetic signal as it would not respond to ground accelerations for which the seismometer is built in the first place.

5.6 Schumann resonances

That the spectrum of magnetic field variations at BFO does not stop at 1 Hz has been demonstrated by our colleagues from ETH Zürich, who operated magnetotelluric sensors for three days in 2016 in the upper Anton tunnel. The spectrum of the induction coils is plotted together with the data from the permanently installed fluxgate and Overhauser magnetometers in fig. 4.1. Burried underneath many narrow technical spectral lines is the broad peak of the lowest-order Schumann

resonance at 7 Hz. This is a standing electromagnetic wave trapped in the wave guide that is formed by an isolator sandwiched between the conducting ionosphere and the conducting solid Earth/Oceans. A wave traveling at the speed of light travels around the globe in 1/7th of a second. This is the simplest explanation of the Schumann resonance at a frequency of ∼7 Hz and its harmonics (14 Hz, 21 Hz). Lightning in tropical thunder storms is thought to be the dominant excitation mechanism for the Schumann resonances (Füllekrug and Constable, 2000).

5.7 Tides

The tides are first of all a phenomenon in the field of gravity. But secondary tidal effects also show up in many neighboring disciplines. Here we show an example from geomagnetism. A plot of the power spectral density of 3.5 years of FGE magnetometer data from BFO is shown in fig. 5.6. The spectral peak at the semi-diurnal lunar frequency M2 of 1.932 cycles per day (cpd) is a sure sign that tidal gravity is at work. For the much larger peaks at the frequencies of the solar harmonics this conclusion cannot be drawn: solar heating of the ionosphere could equally (and more likely) be responsible for these lines.

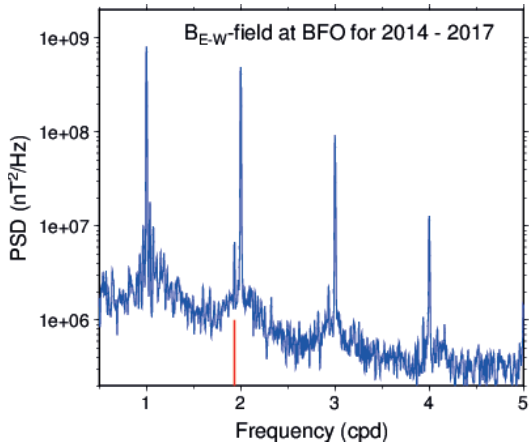

Figure 5.6: Spectrum of the E-W component of magnetic field variations at BFO covering the years 2014 - 2017. The dominant spectral lines are the daily harmonics S1, S2, S3, S4 which are primarily a result of the *Sq* field variations which are generated by the day side, inospheric electric current systems. Indicated with a vertical red line is the semidiurnal lunar tide M2 at 1.932 cycles per day.

So far we can only speculate as to the physical mechanism responsible for the M2 spectral line in the magnetometer data. A first model invokes tidal forcing of the motion in the conducting ionosphere. A second model invokes tidal forcing of the oceans. Since sea water is an electrical conductor an electric current will be induced as it moves through the magnetic field. This electric current in the oceans will be modulated by the dominant tidal frequency, M2. The prime suspect are the ocean tides in the North Sea. At BFO we would observe the *B*-field associated with the induced electric current.

5.8 Outlook: aerspectives for sensors to increase the observed bandwidth

To be compliant with the INTERMAGNET standard we record the magnetic field variations once per second. The comparison of simultaneously recorded signal spectra in fig. 4.1 however shows that for periods shorter than 30 seconds the fluxgate and the Overhauser sensors cannot resolve ambient background variations: the spectra from the induction coils plot below the fluxgate spectra. For frequencies above 0.01 Hz induction coils are preferable: their self-noise is below the level of the ambient field up to at least 1kHz.

How to fuse the data from fluxgates and induction coils into a single record of the magnetic field has been discussed in Brunke et al. (2017). With their suggested procedure it is possible to fill the entire frequency band covered by INTERMAGNET observatory data with usable signal, also between 0.03 and 0.5 Hz. To permanently install and operate a set of three orthogonal induction coils would thus be an obvious addition to expand the covered frequency band at BFO.

5.9 Data access

The magnetics data from BFO are published by INTERMAGNET at `www.intermagnet.org` and by the IRIS/DMC at `http://www.iris.edu`. The data distributed by the IRIS/DMC are the raw output from the Q330 digitizer while INTERMAGNET publishes postprocessed magnetic field values. This postprocessing involves the estimation of a model for the variometer baseline drift for which the DI-flux absolute measurements are needed. The baselines are then added to the calibrated FGE variometer data (see eq. 5.2) to yield a complete description of the magnetic field vector $\vec{B}$. Understandably the delay behind real-time for INTER-

MAGNET data is measured in weeks and months and not in seconds as with the IRIS/DMC.

Acknowledgements

We thank Martin Feller and Martin Beblo from Fürstenfeldbruck Geomagnetic Observatory (FUR) for their continued support with the magnetometer installation and operation at BFO. The technical expertise with magnetic sensors of Eberhard Pulz and the help in becoming an INTERMAGNET observatory from Achim Linthe - both from Niemegk observatory (NGK) is greatly acknowledged. Jürgen Matzka also from NGK has recently taken over the post-processing of magnetics data from BFO for which we are very grateful. Friedemann Samrock and Johannes Käufl from ETH Zürich temporarily operated an MT station in the upper tunnel of the Anton mine consisting of two pairs of electrodes to record the E-field and three induction coils to record the B-field . They kindly provided the data used in fig. 4.1. Klaus Lindner (GIK, KIT) established the geographic reference points needed for the inclination and declination observations.

To work at the Black Forest Observatory is a big privilege: a place where such diverse geophysical phenomena as touched in this paper show up in the locally collected data: the dynamo in the outer core and its secular variations, the Schumann resonances in the electrically isolating spherical shell between ionosphere and solid Earth, the S_q day-side magnetic variations from current systems in the ionosphere, magnetic storms from solar coronal mass ejections (CMEs), the harmonic magnetic field variations at the frequency of the semi-diurnal lunar tide possibly from tidal currents in the North Sea to mention just a few. Bernhard Heck has, in his position as director of the observatory, created an environment in which we as researchers and technicians at BFO could dedicate our time to the study of these signals and the maintenance of the sensors that record them. Bernhard has represented BFO towards the outside and made sure that when needed the concerns of the observatory were heard by the university administrations and even the government of Baden-Württemberg. Thank you, Bernhard!

References

Brunke, H.-P., Widmer-Schnidrig, R., and Korte, M. (2017): Merging fluxgate and induction coil data to produce low-noise geomagnetic observatory data meeting the INTERMAGNET definitive 1 s data standard. *Geosci. Instrum. Method. Data Syst.* 2017. DOI: https://doi.org/10.5194/gi-6-1-2017.

Forbriger, T. (2011): Technical report: Buffer amplifier to connect the SG-056 to a Q330HR recording system. Tech. rep. URL: http://nbn-resolving.org/urn:nbn:de:swb:90-741065.

Forbriger, T. (2013): Technical Documentation: FO-transmission of a 1 PPS signal. Tech. rep. URL: http://nbn-resolving.org/urn:nbn:de:swb:90-360949.

Forbriger, T. (2007): Reducing magnetic field induced noise in broad-band seismic recordings. *Geophys. J. Int.* 169:240–258.

Forbriger, T., Widmer-Schnidrig, R., Wielandt, E., Hayman, M., and Ackerley, N. (2010): Magnetic field background variations can limit the resolution of seismic broad-band sensors. *Geophys. J. Int.* 183:303–312.

Füllekrug, M. and Constable, S. (2000): Global triangulation of intense lightning discharges. *Geophys. Res. Lett.* 27:333–336.

Häfner, R. and Widmer-Schnidrig, R. (2012): Signature of 3-D density structure in spectra of the spheroidal free oscillation ${}_0S_2$. *Geophysical Journal International* 169:240–258. DOI: 10.1093/gji/ggs013.

Hanka, W., Heinloo, A., and Jäckel, K.-H. (2000): Networked seismographs: GEOFON real-time data distribution. *ORFEUS Newsl.* 2. URL: http://www.xn--orfeuseu-5m3d.org/Organization/Newsletter/vol2no3/geofon.html.

Hanka, W., Saul, J., Weber, B., Becker, J., Harjadi, F., and GITEWS Seismology Group (2010): Real-time earthquake monitoring for tsunami warning in the Indian Ocean and beyond. *Nat. Hazards Earth Syst. Sci.* 10.

Jankowski, J. and Socksdorff, C. (1996): Guide for magnetic measurements and observatory practice. International Association for Geomagnetism and Aeronomy, Warsaw.

Klinge, K., Kroner, C., and Zürn, W. (2002): Broadband seismic noise at Stations of the GRSN. In: Korn, M. *Ten years of German Regional Seismic Network (GRSN)*. Weinheim: Wiley-VCH, pp. 83–101.

Van Camp, M., Steim, J., Rapagnani, G., and Rivera, L. (2008): Connecting a Quanterra data logger Q330 on the GWR C021 superconducting gravimeter. *Seismol. Res. Lett.* 79:786–796.

Wielandt, E. (2012): Seismometer calibration with program CALEX. In: Bormann, P. *New Manual of Seismological Observatory Practice 2 (NMSOP-2), Exercise 5.4*. Potsdam, Germany: GeoForschungsZentrum GFZ, pp. 1–51. DOI: 10.2312/GFZ.NMSOP-2_EX_5.4.

Wielandt, E. and Forbriger, T. (2016): Linux version of program CALEX. URL: https://git.scc.kit.edu/Seitosh/software-for-seismometry-linux/tree/master/software/calex.